Research Square

Preprints are preliminary reports that have not undergone peer review.
They should not be considered conclusive, used to inform clinical practice,
or referenced by the media as validated information.

Influence of the Area of the Aqueduct on Quantification of Stroke Volume and Max Velocity in Healthy Volunteers Using Phase Contrast Cine MRI

hongri zhang (hongrizhang1978@yeah.net)
Henan University of Science and Technology https://orcid.org/0000-0003-3269-8127
Weike Duan
Henan University of Science and Technology Affiliated First Hospital
Xiaopan Li
Henan University of Science and Technology Affiliated First Hospital
Yixin Wang
Fred Hutchinson Cancer Research Center
Xinyu Li
Henan University of Science and Technology Affiliated First Hospital
Petrice Mostardi M. Cogswell
Mayo Clinic: Mayo Clinic Minnesota
Benjamin D D. Elder
Mayo Clinic: Mayo Clinic Minnesota

Research

Keywords: CSF dynamics, aqueduct, region of interest, magnetic resonance imaging, CSF stroke volume, velocity

Posted Date: March 24th, 2021

DOI: https://doi.org/10.21203/rs.3.rs-334057/v1

License: This work is licensed under a Creative Commons Attribution 4.0 International License.
Read Full License

Abstract

Background: The relationship of the area of the aqueduct on quantification of the aqueductal stroke volume (SV) and max velocity need further investigation. Our aim was to assess the influence of the area of the aqueduct on quantification of the aqueductal SV and max velocity measured with phase contrast magnetic resonance imaging (PC-MRI) within the cerebral aqueduct at the level of the intercollicular sulcus.

Materials and Methods: Nine healthy volunteers (mean age 29.6 yrs) were enrolled in the study and brain MRIs were performed on a 3.0T system. Quantitative analysis of aqueductal cerebrospinal fluid (CSF) flow was performed using manual regions of interest (ROI) placement. ROIs were separately drawn for each of 12 phases of the cardiac cycle, and changes in aqueduct size during the cardiac cycle were determined. Stroke volumes were calculated uses the first and ninth aqueductal ROIs and compared to each other. Max velocities at the 12 phases were also collected, and the relationship between the area and max velocity and the impact on SV were analyzed.

Results: There was variation in the size of the aqueduct during the cardiac cycle, the first area (S1) was larger than the ninth (S9). The first max velocity (Vmax1) was less than the ninth (Vmax9). Additionally, there was a significant different between the stroke volume calculated using the first aqueductal ROI (SV1) and the ninth (SV9).

Conclusions: There is variation in the size of the cerebral aqueduct which is used to calculate stroke volume and other CSF flow parameters during the cardiac cycle. The maximum velocity may be inversely proportional to the area of the aqueduct. In order to establish reliable reference values for CSF flow parameters in future studies, a variable ROI, to account for cardiac cycle variation, should be considered and incorporated.

Introduction

Phase contrast cine magnetic resonance imaging (PC-MRI) has been used to measure cerebrospinal fluid (CSF) flow dynamics. Stroke volume is defined as the net flow of CSF in a defined region of interest (ROI), and is often measured in the cerebral aqueduct. [1–5] Previous studies have evaluated CSF flow in healthy subjects as well as pathological flow in hydrocephalus [1, 6, 7, 8], aqueduct obstructions[9], Chiari malformation[10], and interventions[11, 12]. PC-MRI has also has been used to evaluate the patency of third ventriculostomies as well as shunt catheter flow[13–15].

As the CSF flow parameters are calculated, they depend on different factors such as specific MR machine, field strength, sequence parameters, post processing software [4], as well as patient age and gender [16]. Additionally, aqueduct area may change with age, disease and intracranial pressure (ICP) [17], but its change has not been assessed with the cardiac cycle.

As we know, the blood flow velocity is inversely proportional to the cross-sectional area of the blood vessel. Karin Markenroth Bloch et al. [18] reported that the maximum velocity-time curve of CSF in the aqueduct was similar to the blood flow velocity curve in a cardiac cycle. As our study found that there was variation in the size of the aqueduct during the cardiac cycle, there is a hypothesis that the CSF flow velocity is inversely proportional to the size of aqueduct, so we try to prove it.

Furthermore, despite the development of several semiautomated segmentation methods [19, 20], manual ROI segmentation is still widely used [1–18]. Although quantitative assessments of stroke volume have been conducted at the aqueductal level, current calculation methods only select a static area of ROI, so there is limited data on the impact of changes in area of the aqueductal ROI on stroke volume. Therefore, the objective of this study was to determine how much the size of the aqueduct varied during the cardiac cycle and how ROI size affects the calculated stroke volume measured by PC-MRI.

Materials And Methods

Participants

The study protocol was approved by the local Ethics Committee and informed consent was obtained from all participants. Nine healthy volunteers were identified and enrolled in the study. Subjects with a cardiac arrhythmia were excluded from the study.

MR Acquisition

PC-MRI was performed using a 3.0-T MRI scanner (Phillips Achieva 3.0T TX, The Netherlands) with a 16-channel head coil and MR Extended Workspace R2.6.3.5 station (Philips, The Netherlands). A routine clinical protocol was used to obtain T1-weighted (T1w), T2w and T2w FLAIR images. Product sequences, CSF-QF sequences were then used to analyze CSF flow. The following imaging parameters were used: minimum TR and TE, flip angle = 15°, FOV = 150 mm * 150 mm, matrix = 256 * 256, slice thickness = 4 mm; flow direction from feet to head; velocity encoding value was 12cm/s. The acquisition time was 3–6 min, based on the participant's heart rate. A single slice was acquired with plane orthogonal to the aqueduct at the level of the intercollicular sulcus (Fig. 1). Retrospective cardiac gating via peripheral pulse device, known as peripheral pulse triggering, was performed. The data was binned into 12 phases during a cardiac cycle, based on the R-R interval. CSF flow was quantitatively analyzed with software (CSF-QF). The velocity versus time curve should be nearly sinusoidal with a period equal to the R-R interval in the ECG. [5, 14]

Analysis

We first sought to measure the change in area of the aqueduct during a cardiac cycle. All 12 scans in a cardiac cycle were extracted, and in each image, the ROI was drawn by two attending radiologists, to enclose the aqueduct with as little surrounding tissue as possible (Fig. 2A). Next, the area enclosed within

each ROI was measured (Fig. 2B). The variation in ROI in the 12 images over the cardiac cycle is depicted in Fig. 2C.

Next, 12 maximum velocities were collected after scan, as demonstrated in Fig. 2B.

Because we found that the aqueductal area of the first scan(which was defined as A_1) was larger than the ninth(which was defined as A_9) statistically significant, then the first max velocity(V_{max1})were chose to compare with the ninth（V_{max9}）.

Lastly, the SV was recalculated based on a dynamic ROI. The first area ROI from each cardiac cycle was used to calculate the first SV, which was defined as SV_1. Similarly, the ninth area ROI was used to calculate the ninth SV, defined as SV_9. Then compare SV_1 with SV_9. The specific process is shown in Fig. 3.

Statistical analysis

SPSS ver. 19.0 software (SPSS, Inc., Chicago, IL, USA) and R ver. 3.6.0 software were used for the statistical analysis. All data were presented as the mean ± standard deviation (SD). To analyze the change in area and maximum velocity of the aqueduct during a cardiac cycle, the change in area and maximum velocity of the 12 observations for each patient was defined as the difference between the area and maximum velocity at each timepoint and the initial ROI area. A t-test with a Bonferroni correction was then applied to compare the variation in ROI area and maximum velocity with time, separately. Applying Bonferroni correction, $P = 0.05$ was divided by the number of tests (11) to get the Bonferroni critical value, with $P < 0.05/11$ defined as significant.

The student's t-test was used to compare A_1 vs A_9, V_{max1} vs V_{max9}, SV_1 vs SV_9. A *P*-value of < 0.05 was considered statistically significant.

Results

The nine volunteers included four men and five women age reange 21–57 yrs, mean ± std 29.6 ± 9.1 yrs. All patients had no prior history of neurologic disease, no cerebrovascular disorders, and no medication use.

The aqueduct was scanned 12 times during a cardiac cycle, based on the R-R interval. The changes in area of the aqueduct throughout the cardiac cycle are displayed in Table 1. *P* value at each time point is shown in the last column of the table below, and 3 of them show a significant *P* value ($P < 0.05$). After Bonferroni correction was applied, the difference between the measures at the ninth time point and the first time point is significant ($P < 0.05/11$). (Table 1,Fig. 4)

Table 1
T test for the Change in Area of the Aqueduct of the Nine Patients at Each Observation Time in a Cardiac Cycle

Time	Pt 1	Pt 2	Pt 3	Pt 4	Pt 5	Pt 6	Pt 7	Pt 8	Pt 9	Mean	P value
2	-14	-6	7	0	0	4	0	-14	-14	-4.1	0.171
3	-18	-10	-7	0	3	0	-14	0	-17	-7.0	0.032
4	-17	0	-11	-21	10	0	-14	-4	-10	-7.4	0.052
5	-24	4	-4	-7	3	-7	-3	0	-10	-5.3	0.094
6	-20	7	-7	-7	10	0	-7	3	-10	-3.4	0.301
7	-14	7	3	0	10	4	3	-7	0	0.7	0.790
8	-20	-10	-7	0	0	-10	-3	-4	3	-5.7	0.042
9	-25	-17	-11	-14	-11	-10	-21	10	-21	-13.3	0.004
10	-24	-20	-7	-14	13	0	0	10	-7	-5.4	0.231
11	-17	-13	7	-7	0	4	0	0	-14	-4.4	0.159
12	-17	-13	0	-7	3	4	0	0	-14	-4.9	0.104

The changes of maximum velocity in the aqueduct throughout the cardiac cycle are displayed in Table 2. *P* value at each time point is shown in the last column of the table below, and 8 of them show a significant ($P < 0.05$) *P* value. Applying the Bonferroni correction, $P = 0.05$ is divided by the number of tests (11) to get the Bonferroni critical value, so a test would have to have $P < 0.05/11$ to be significant. Under this criterion, the tests at time 4, 5, 6, 9, 10, 11, 12 are significant. Therefore, we could reject the hypothesis that there are no differences between the speeds at the following time points and the first time point. (Table 2,Fig. 5)

Table 2
T test for the Change in Max Velocity of the Nine Patients at Each Observation Time in a Cardiac Cycle

Time	ptid1	ptid2	ptid3	ptid4	ptid5	ptid6	ptid7	ptid8	ptid9	Mean	p-value
2	-0.1	-2.2	1.1	0	-0.9	0.6	-3.0	1.0	0.3	-0.3	0.494
3	1.7	-1.9	2.7	-0.1	1.7	3.4	-1.2	3.1	2.0	1.3	0.079
4	4.4	0.3	3.8	1.1	4.7	4.7	2.0	5.0	3.3	3.3	0
5	5.7	1.6	4.0	1.9	5.9	6.0	4.4	3.8	3.4	4.1	0
6	6.1	2.2	2.9	2.0	6.1	6.3	6.0	0.2	3.6	3.9	0.001
7	2.5	0.1	1.5	0.1	5.2	2.2	4.9	1.7	3.1	2.4	0.005
8	0.2	-2.3	4.0	0.3	2.3	1.9	-1.2	3.2	0.2	1.0	0.201
9	5.9	0.3	4.7	2.0	5.3	6.9	2.0	3.8	4.4	3.9	0.001
10	9.0	2.9	3.2	2.2	6.5	8.3	5.7	2.7	7.8	5.4	0
11	6.2	2.5	1.2	1.5	4.5	5.2	5.4	1.3	5.8	3.7	0.001
12	2.7	1.4	0.1	0.9	1.5	1.9	2.9	0.2	2.7	1.6	0.002

The results of this study showed that V_{max1} was significantly lower than V_{max9}(-1.16 ± 1.89 vs -5.77 ± 1.89 P = 0.001) (Fig. 6). Compare with S1 and S9,the difference is significant(81.56 ± 20.17 vs 68.22 ± 16.02 P = 0.004) (Fig. 7). The results also showed that max velocity is inversely proportional to the area of aqueduct.

The results of this study showed that SV_1 was significantly less than SV_9 (0.0044 ± 0.0034 vs 0.0061 ± 0.0033, P = 0.0282) (Fig. 8).

Discussion

The ROI size affects the mean velocity, flow rate, and SV differently. The flow in the center is higher than that at the periphery, so a small ROI placed in the center of the aqueduct will give higher readings of mean velocity while a larger ROI will underestimate it [24]. The max velocity representing the fastest flow in any pixel in the given ROI is not affected by the ROI size [25]. As a result, we chose maximum velocity for our analysis.

Karin Markenroth Bloch et al [18] reported that the speed curve conforms to the sinusoidal curve. Our results are consistent with his research. This study showed that S_1 is significantly larger than S_9 in a cardiac cycle, as a result, we chose $V_{max1}$and V_{max9} to compare, and we found that the maximum velocity may be inversely proportional to the area of the aqueduct. Dieter R. Enzmann et al [26] reported that the primary driving force behind intracranial and spinal canal CSF flow is expansion of the brain during

vascular systole since arterial inflow and venous outflow are not equal throughout a cardiac cycle, and there is a short period of brain expansion during vascular systole. According to Dieter R. Enzmann's theory, we speculate that the brain tissue expands during the arterial systole and squeezes aqueduct, then aqueduct becomes smaller; at the same time the intracranial pressure increases and the flow rate of cerebrospinal fluid becomes faster. In contrast, during arterial diastole, brain tissue will shrink, the force of the surrounding the aqueduct squeezed by brain tissue is reduced, the area is expanded, while the intracranial pressure is reduced and the flow rate of cerebrospinal fluid is slowed.

SV is an important parameter often used in PC-MRI research, especially in aqueducts. SV is sometimes calculated differently because of the evaluation software chosen. For example, SV was averaged over the diastolic and systolic fluxes in the paper of Bradley et al [11]. Shanks J defined SV as the volumetric mean of the caudal and cranial flow of CSF through the aqueduct [14]. In our study, SV of the aqueduct is equal to the net flow of cerebrospinal fluid during a cardiac cycle (approximately forward flow volume minus backward flow volume), similarly to a prior study by Sartoretti et al [5]. Cerebrospinal fluid flow within the aqueduct is best described as a to-and-fro motion with a very small net flow, and this normal variation is mainly related to the size and anatomy of CSF spaces, systolic and diastolic arterial blood pressure, jugular venous flow, and respiration [27].

In most of the current post processing software, SV is equal to Mean flux (ml/s)×60/ heartbeat (1 RR-interval). = Mean velocity × Area of ROI. Theoretically, mean velocity becomes smaller as the Area of ROI becomes larger, so, mean flux remains unchanged. As a result, various size of manually delineated ROI appeared in many studies[28]. However, some research shows that there remains a considerable inaccuracy in the volume data effected by the placement of the ROI [29, 30, 31], but these studies did not point out specific reasons. The results of this study also show that volume data are affected by the placement of the ROI. Because we choose the area of the aqueduct at different times as a reference for ROI, maybe the reason of volume data affected by the placement of the ROI is related to the change of aqueductal area.

The definition of SV_1 and SV_9 is based on the area of the aqueduct, while the latter is determined by the area of the ROI. Whether SV_1 or SV_9 is closer to the real flow requires further study. Anyway, the difference between SV_1 and SV_9 is significant indicating that volume data are affected by the placement of the ROI. Therefore, we should consider how to define the ROI more accurately when detecting SV. In addition, whether there are other clinical significance remains to be further studied.

Because the flow rate of CSF in the aqueduct is very slow [22]. It is a challenge to quantitatively detect it using PC-MRI. Najafi et al reported that PC-MR was able to quantify low flow rates in vitro (0.1-5 ml/s) with a maximum underestimation of 5–10% [29]. The PC-MR imaging parameters chosen in this study are similar to theirs. Many parameters affect SV. One important parameter of the PC sequence is the VENC. Low VENC demands large gradients, resulting in long TE, which can increase signal loss due to intravoxel dephasing, especially in pathological situations with complex flow [18].The value of the VENC should be

chosen as close to the velocity of the fluid flow encountered in subjects [5]. A relatively high VENC (12 cm/s) was chosen in this study because the subjects presented with peak velocities of around 2-11 cm/s.

This study has several limitations: first, the number of volunteers is small, especially when comparing SV_1 and SV_9, which may affect the results. Secondly, 2D PC-MRI was used in this study, and velocity was encoded in only one spatial direction, which resulted in in-plane velocity images or through-plane flow curves [22]. Because the motion of CSF through the ventricular system is a complex three-dimensional dynamic process, 3D analysis may be more accurate. Third, the effects of some related factors on breathing, sleep, and age have not been analyzed, which maybe have influence on results [5,32,33].

Conclusions

There is variation in the size of the cerebral aqueduct which is used to calculate stroke volume and other CSF flow parameters during the cardiac cycle. The maximum velocity may be inversely proportional to the area of the aqueduct. In order to establish reliable reference values for CSF flow parameters in future studies, a variable ROI, to account for cardiac cycle variation, should be considered and incorporated.

Declarations

Acknowledgements

We thank Xiaobing Cheng and volunteers for assistance in the study.

Authors' contributions

HZ: experiment design and conception, data collection, data analysis, manuscript writing; WD: data analysis, manuscript revision; XPL: data analysis, manuscript revision; YW: data analysis, manuscript revision; XYL: data analysis, manuscript revision; PMC: data analysis, manuscript revision; BDE: experiment design and conception, data collection, data analysis, manuscript revision. All authors read and approved the final manuscript.

Funding

grant sponsor: Henan Province Medical Science and Technology Research Plan; Contract grant number: SB201901066; Contract grant sponsor: The Medical and Manitation of Luoyang Science and Technology Program; Contract grant number: 1722001A-6.

Availability of data and materials

All reasonable requests for data will be gladly granted by the corresponding author.

Ethics approval and consent to participate

The study protocol was approved by the The First Affiliated Hospital of Henan University of Science and Technology Ethics Committee and informed consent was obtained from all participants.

Consent for publication

The authors have all consented to the publication of this manuscript.

Declaration of Conflicting Interests

The author(s) declared no potential conflicts of interest with respect to the research, authorship, and/or publication of this article.

Author information

Department of Neurosurgery, The First Affiliated Hospital of Henan University of Science and Technology, #24 Jinghua Road, Luoyang 471003, China.

Hongri Zhang & Weike Duan

Department of Radiology, The First Affiliated Hospital of Henan University of Science and Technology, #24 Jinghua Road, Luoyang 471003, China.

Xiaopan & LiXinyu Li

Vaccine and Infectious Disease Division, Fred Hutchinson Cancer Research Center, Seattle 98109, USA.

Yixin Wang

Department of Radiology, Mayo Clinic, 200 First St SW, Rochester, MN 55905, USA.

Petrice M. Cogswell

Departments of Neurosurgery, Mayo Clinic, 200 First St SW, Rochester, MN 55905, USA.

Benjamin D. Elder

Departments of Bioengineering, Mayo Clinic, 200 First St SW, Rochester, MN 55905, USA.

Benjamin D. Elder

Departments of Orthopedics, Mayo Clinic, 200 First St SW, Rochester, MN 55905, USA.

Benjamin D. Elder

*Corresponding author

Correspondence to Benjamin D. Elder. elder.benjamin@mayo.edu Departments of Neurosurgery, Mayo Clinic, 200 First St SW, Rochester, MN 55905, USA.

Abbreviations

ROI = region of interest; SV = stroke volume; PC-MRI = phase contrast magnetic resonance imaging; CSF = cerebrospinal fluid; VENC = velocity encoding value; ICP = intracranial pressure

References

[1]. Enzmann DR, Pelc NJ. Normal flow patterns of intracranial and spinal cerebrospinal fluid defined with phase-contrast cine MR imaging. *Radiology* 1991;178(2):467-74. doi:10.1148/radiology.178.2.1987610

[2]. Luetmer PH, Huston J, Friedman JA, Dixon GR, Petersen RC, Jack CR, et al. “Measurement of Cerebrospinal Fluid Flow at the Cerebral Aqueduct by Use of Phase-Contrast Magnetic Resonance Imaging: Technique Validation and Utility in Diagnosing Idiopathic Normal Pressure Hydrocephalus.” *Neurosurgery* 2002;50(3):534-543-544. doi:10.1097/00006123-200203000-00020.

[3]. Battal B, Kocaoglu M, Bulakbasi N, Husmen G, Tuba Sanal H, Tayfun C. “Cerebrospinal Fluid Flow Imaging by Using Phase-Contrast MR Technique.” *The British Journal of Radiology* 2011;84(1004):758–65. doi:10.1259/bjr/66206791.

[4]. Bradley WG. “CSF Flow in the Brain in the Context of Normal Pressure Hydrocephalus.” *American Journal of Neuroradiology* 2015;36(5):831–38. doi:10.3174/ajnr.A4124.

[5]. Sartoretti T, Wyss M, Sartoretti E, Sartoretti E, Reischauer C, Hainc N, Grafet N, et al. Sex and Age Dependencies of Aqueductal Cerebrospinal Fluid Dynamics Parameters in Healthy Subjects. *Front Aging Neurosci* 2019;11:199. doi:10.3389/fnagi.2019.00199.

[6]. Nitz WR, Bradley WG, Watanabe AS, Lee RR, Burgoyne B, O'Sullivan RM,et al. Flow dynamics of cerebrospinal fluid: assessment with phase-contrast velocity MR imaging performed with retrospective cardiac gating. *Radiology* 1992;183:395–405. doi: 10.1148/radiology.183.2.1561340

[7]. Gideon P, Ståhlberg F, Thomsen C, Gjerris F, Sørensen PS, Henriksen O. Cerebrospinal fluid flow and production in patients with normal pressure hydrocephalus studied by MRI. *Neuroradiology* 1994;36:210–215. doi:10.1007/BF00588133

[8].Gokul UR, Ramakrishnan KG. Change in average peak cerebrospinal fluid velocity at the cerebral aqueduct, before and after lumbar CSF tapping by the use of phase contrast MRI, and its effect on gait improvement in patients with normal pressure hydrocephalus. *Neurol India* 2018;66(5):1407-1412. doi:10.4103/0028-3886.241406.

[9]. Muehlmann M, Koerte IK, Laubender RP, Steffinger D, Lehner M, Peraud A,et al. Magnetic resonance-based estimation of intracranial pressure correlates with ventriculoperitoneal shunt valve opening pressure setting in children with hydrocephalus. *Invest Radiol* 2013;48:543–547. doi:10.1097/RLI.0b013e31828ad504.

[10]. Alperin N, Kulkarni K, F Loth, Roitberg B, Foroohar M, Mafeeet MF, et al. Analysis of magnetic resonance imaging–based blood and cerebrospinal fluid flow measurements in patients with Chiari I malformation: a system approach. *Neurosurg Focus* 2001;11(1):E6. doi:10.3171/foc.2001.11.1.7.

[11].Bradley WG, Scalzo D, Queralt J, Nitz WN, Atkinson DJ, Wong P. Normal-pressure hydrocephalus: evaluation with cerebrospinal fluid flow measurements at MR imaging. *Radiology* 1996;198:523–529. doi:10.1148/radiology.198.2.8596861.

[12].Kahlon B, Annertz M, Stahlberg F, Rehncrona S. Is aqueductal stroke volume, measured with cine phase-contrast magnetic resonance imaging scans useful in predicting outcome of shunt surgery in suspected normal pressure hydrocephalus? *Neurosurgery* 2007;60:124–130. doi:10.1227/01.NEU.0000249208.04344.A3.

[13]. Wymer DT, Patel KP, Burke WF 3rd, Bhatia VK. Phase-Contrast MRI: Physics,Techniques, and Clinical Applications. *Radiographics* 2020;40(1):122-140. doi:10.1148/rg.2020190039.

[14]. Shanks J, Markenroth Bloch K, Laurell K, Cesarini KG, Fahlström M, Larsson EM, et al. Aqueductal CSF Stroke Volume Is Increased in Patients with Idiopathic Normal Pressure Hydrocephalus and Decreases after Shunt Surgery. *Am J Neuroradiol* 2019;40(3):453-459. doi:10.3174/ajnr.A5972.

[15]. Jakimovski D, Zivadinov R, Weinstock-Guttman B, Bergsland N, Dwyer MG, Laganaet MM. Longitudinal analysis of cerebral aqueduct flow measures: multiple sclerosis flow changes driven by brain atrophy. *Fluids Barriers CNS* 2020;17(1):9. doi:10.1186/s12987-020-0172-3.

[16]. Daners MS, Knobloch V, Soellinger M, Boesiger P, Seifert B, Guzzella L, et al. “Age-Specific Characteristics and Coupling of Cerebral Arterial Inflow and Cerebrospinal Fluid Dynamics.” *PLOS ONE* 2012;7(5):e37502. doi:10.1371/journal.pone.0037502.

[17]. Long J, Lin H, Cao G, Wang MZ, Huang X, Xia J, et al. Relationship between intracranial pressure and phase-contrast cine MRI-derived measures of cerebrospinal fluid parameters in communicating hydrocephalus. *Quant Imaging Med Surg*. 2019;9(8):1413-1420. doi:10.21037/qims.2019.08.04

[18]. Markenroth Bloch K, Töger J, Ståhlberg F. Investigation of cerebrospinal fluid flow in the cerebral aqueduct using high-resolution phase contrast measurements at 7T MRI. *Acta Radiol* 2018;598(8). doi:10.1177/0284185117740762

[19]. Yoshida K, Takahashi H, Saijo M, Ueguchi T, Tanaka H, Fujita N, et al. Phase-contrast MR studies of CSF flow rate in the cerebral aqueduct and cervical subarachnoid space with correlation-based segmentation. *Magn Reson Med Sci* 2009;8(3):91-100.doi:10.2463/mrms.8.91.

[20]. Flórez YN, Moratal D, Forner J, Martí-Bonmatí L, Arana E, Guajardo-Hernández U, et al. Semiautomatic analysis of phase contrast magnetic resonance imaging of cerebrospinal fluid flow through the aqueduct of Sylvius. *MAGMA* 2006;19:78–87. doi:10.1007/s10334-006-0030-6

[21]. Chiang WW, Takoudis CG, Lee SH, Weis-McNulty A, Glick R, Alperin N. Relationship between ventricular morphology and aqueductal cerebrospinal fluid flow in healthy and communicating hydrocephalus. *Invest Radiol* 2009;44:192–199. doi:10.1097/RLI.0b013e31819a640b.

[22]. Stadlbauer A, Salomonowitz E, Brenneis C, Ungersböck K, Riet W, Buchfelderet M et al. Magnetic resonance velocity mapping of 3D cerebrospinal fluid flow dynamics in hydrocephalus: preliminary results. *Eur Radiol* 2012;221(1). doi:10.1007/s00330-011-2247-7

[23]Holmlund P, Qvarlander S, Malm J, Eklund A. Can pulsatile CSF flow across the cerebral aqueduct cause ventriculomegaly? A prospective study of patients with communicating hydrocephalu. *Fluids Barriers CNS* 2019;16(1):40. doi:10.1186/s12987-019-0159-0.

[24]. Tawfik AM, Elsorogy L, Abdelghaffar R, Naby AA, Elmenshawi I. Phase-Contrast MRI CSF Flow Measurements for the Diagnosis of Normal-Pressure Hydrocephalus: Observer Agreement of Velocity Versus Volume Parameters. *Am J Roentgenol* 2017;208(4):838-843. doi:10.2214/AJR.16.16995.

[25]. Sharma AK, Gaikwad S, Gupta V, Garg A, Mishra NK. Measurement of peak CSF flow velocity at cerebral aqueduct, before and after lumbar CSF drainage, by use of phase-contrast MRI: utility in the management of idiopathic normal pressure hydrocephalus. *Clin Neurol Neurosurg* 2008;110:363–368. doi:10.1016/j.clineuro.2007.12.021

[26]. Enzmann DR, Pelc NJ. Cerebrospinal Fluid Flow Measured by Phase-Contrast Cine MR. *Am J Neuroradiol* 1993;146(6).

[27]. Quencer RM, Donovan Post MJ, Hinks RS. Cine MR in the evaluation of normal and abnormal CSF flow: intracranial and intraspinal studies. *Neuroradiology* 1990;32:371–391. doi:10.1007/BF00588471.

[28] Schroeder C, Fleck S, Gaab MR, Schweim KH, Schroederet HWS. Why does endoscopic aqueductoplasty fail so frequently? Analysis of cerebrospinal fluid flow after endoscopic third ventriculostomy and aqueductoplasty using cine phase-contrast magnetic resonance imaging. *J Neurosurg* 2012;117(1):141-9. doi:10.3171/2012.3.

[29]. Najafi A, Sartoretti TDJ, Binkert CA, Sartoretti-Schefer S, Wyss M. CSF flow quantification in the cerebral aqueduct using phase contrast MR-How to do it properly. *European Society of Radiology* 2018;C-1577. doi:10.1594/ecr2018/C-1577

[30].Kapsalaki E, Svolos P, Tsougos I, Theodorou K, Fezoulidis I, Fountas KN. Quantification of normal CSF flow through the aqueduct using PC-cine MRI at 3T. *Acta Neurochir Suppl (Wien)* 2012;113:39–42. doi:10.1007/978-3-7091-0923-6_8

[31]. Lee JH, Lee HK, Kim JK, Kim HJ, Park JK, Choi CG. CSF flow quantification of the cerebral aqueduct in normal volunteers using phase contrast cine MR imaging. *Korean J Radiol* 2004;52(2). doi:10.3348/kjr.2004.5.2.81

[32]. Vinje V, Ringstad G, Lindstrøm EK, Valnes LM, Rognes ME, Eide PK, et al. Respiratory influence on cerebrospinal fluid flow – a computational study based on long-term intracranial pressure measurements. *Sci Rep* 2019;9(1):9732. doi:10.1038/s41598-019-46055-5.

[33]. Nilsson C, Ståhlberg F, Thomsen C, Henriksen O, Herning M, Owman C. Circadian variation in human cerebrospinal fluid production measured by magnetic resonance imaging. *Am J Physiol* 1992;262(1 Pt 2): R20-4. doi:10.1152/ajpregu.1992.262.1. R20.

Tables

TABLE 1. T test for the Change in Area of the Aqueduct of the Nine Patients at Each Observation Time in a Cardiac Cycle

Time	Pt 1	Pt 2	Pt 3	Pt 4	Pt 5	Pt 6	Pt 7	Pt 8	Pt 9	Mean	P value
2	-14	-6	7	0	0	4	0	-14	-14	-4.1	0.171
3	-18	-10	-7	0	3	0	-14	0	-17	-7.0	0.032
4	-17	0	-11	-21	10	0	-14	-4	-10	-7.4	0.052
5	-24	4	-4	-7	3	-7	-3	0	-10	-5.3	0.094
6	-20	7	-7	-7	10	0	-7	3	-10	-3.4	0.301
7	-14	7	3	0	10	4	3	-7	0	0.7	0.790
8	-20	-10	-7	0	0	-10	-3	-4	3	-5.7	0.042
9	-25	-17	-11	-14	-11	-10	-21	10	-21	-13.3	0.004
10	-24	-20	-7	-14	13	0	0	10	-7	-5.4	0.231
11	-17	-13	7	-7	0	4	0	0	-14	-4.4	0.159
12	-17	-13	0	-7	3	4	0	0	-14	-4.9	0.104

TABLE 2. T test for the Change in Max Velocity of the Nine Patients at Each Observation Time in a Cardiac Cycle

ime	ptid1	ptid2	ptid3	ptid4	ptid5	ptid6	ptid7	ptid8	ptid9	Mean	p-value
	-0.1	-2.2	1.1	0	-0.9	0.6	-3.0	1.0	0.3	-0.3	0.494
	1.7	-1.9	2.7	-0.1	1.7	3.4	-1.2	3.1	2.0	1.3	0.079
	4.4	0.3	3.8	1.1	4.7	4.7	2.0	5.0	3.3	3.3	0
	5.7	1.6	4.0	1.9	5.9	6.0	4.4	3.8	3.4	4.1	0
	6.1	2.2	2.9	2.0	6.1	6.3	6.0	0.2	3.6	3.9	0.001
	2.5	0.1	1.5	0.1	5.2	2.2	4.9	1.7	3.1	2.4	0.005
	0.2	-2.3	4.0	0.3	2.3	1.9	-1.2	3.2	0.2	1.0	0.201
	5.9	0.3	4.7	2.0	5.3	6.9	2.0	3.8	4.4	3.9	0.001
0	9.0	2.9	3.2	2.2	6.5	8.3	5.7	2.7	7.8	5.4	0
1	6.2	2.5	1.2	1.5	4.5	5.2	5.4	1.3	5.8	3.7	0.001
2	2.7	1.4	0.1	0.9	1.5	1.9	2.9	0.2	2.7	1.6	0.002

Figures

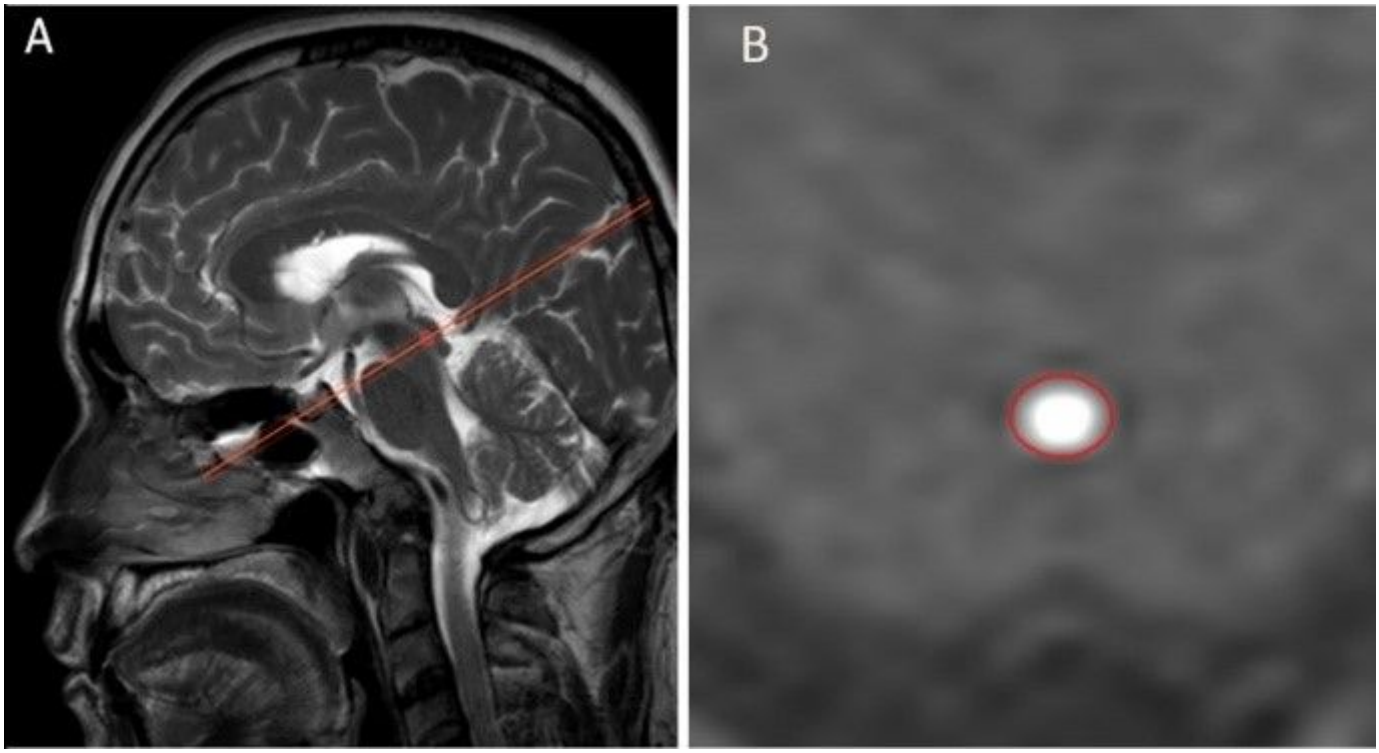

Figure 1

Illustration of slice positioning. A: Sagittal T2-weighted scout MR image showing the phase-contrast imaging plane perpendicular to the aqueduct (red line) for assessing CSF flow. B: Axial phase-contrast image perpendicular to the aqueduct showing an annular ROI around the aqueduct.

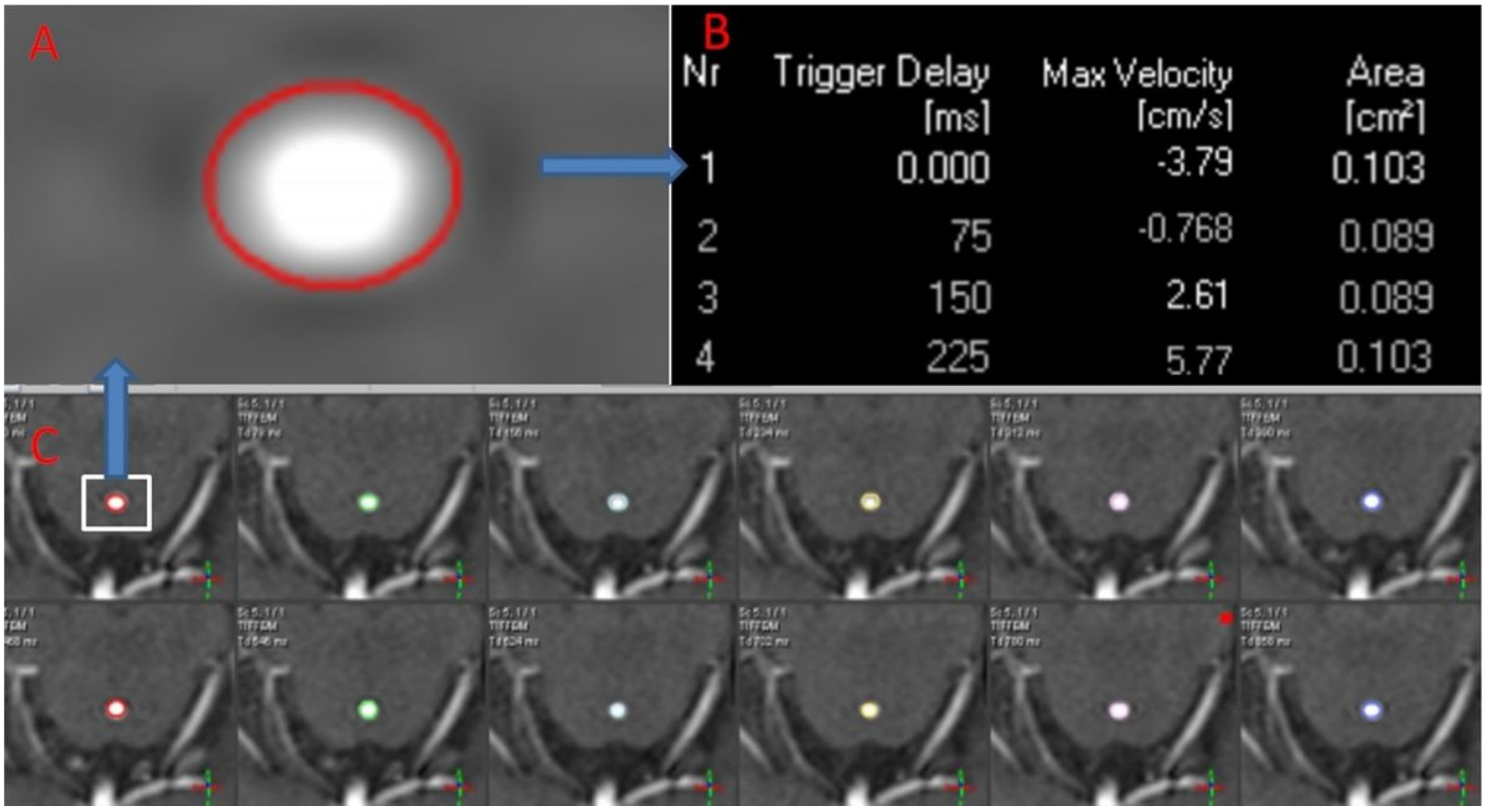

Figure 2

Change in aqueduct size during a cardiac cycle. A: ROI was drawn and it was enclosed the aqueduct with as little surrounding tissue as possible. B: The aqueduct Area and Max Velocity of each scan was automatic calculated. C: All of ROI were drawn with the same criterion.

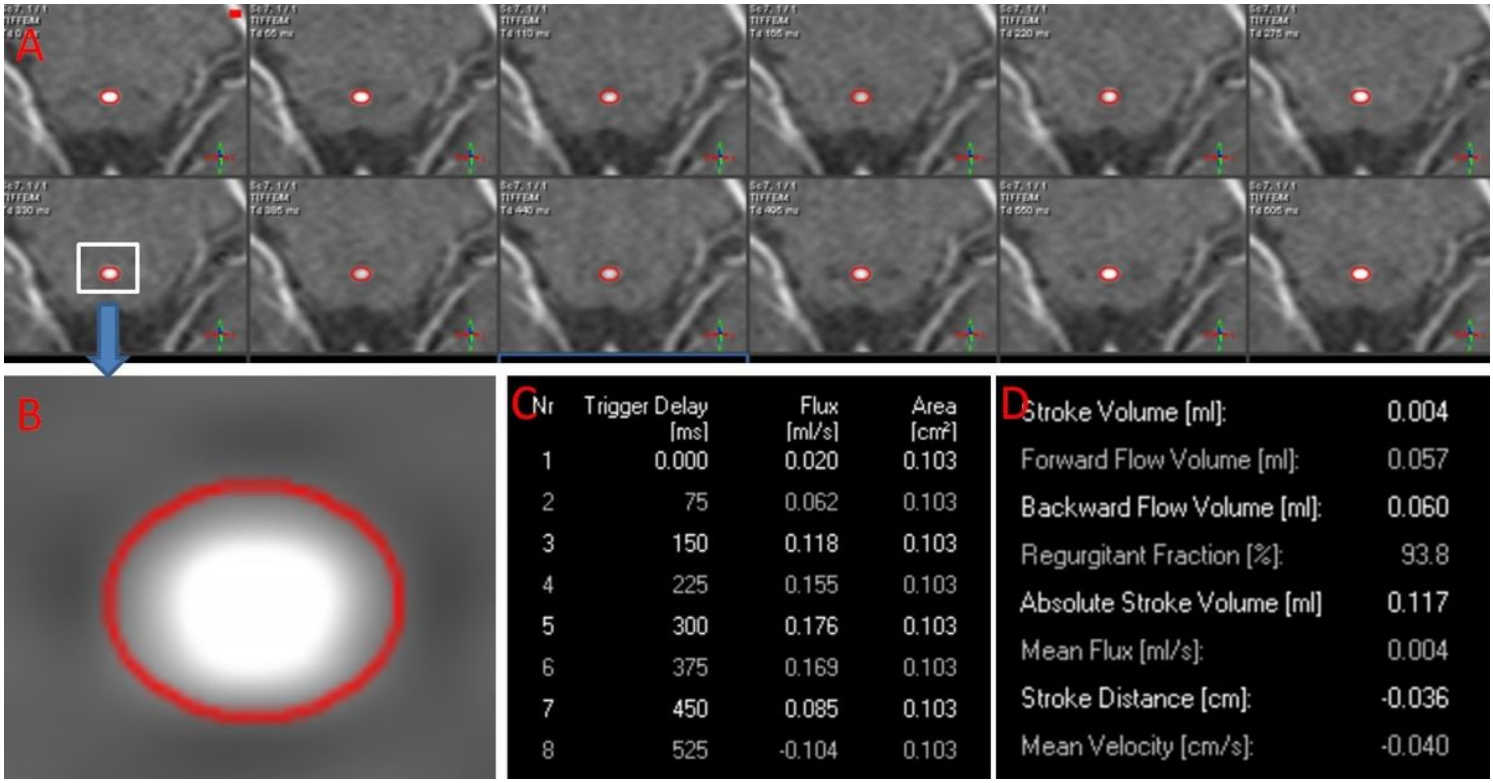

Figure 3

Illustration of stroke volume measured with different ROI areas, fixed over the course of the cardiac cycle. A: All of ROI were the same according to area we chose. B: ROI was drawn around the center of the aqueduct. C: The areas of all scanned are the same. D: Parameters of absolute stroke volume (ml), forward flow volume (ml), backward flow volume (ml), regurgitation fraction, mean flux (ml / sec), stroke distance (cm), mean velocity (cm / sec) are show with one ROI area.

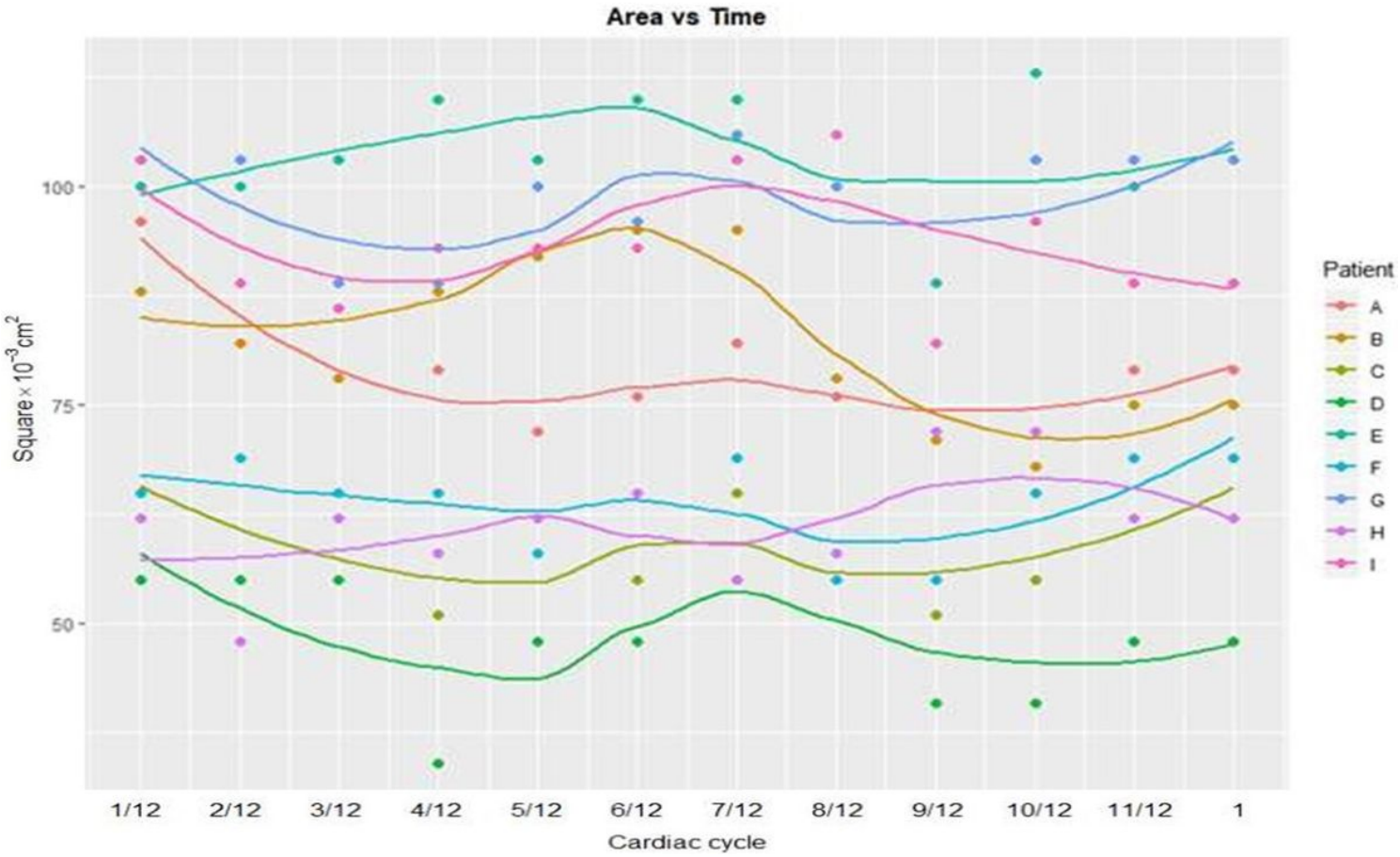

Figure 4

Illustration of the changes in area of the aqueduct throughout the cardiac cycle

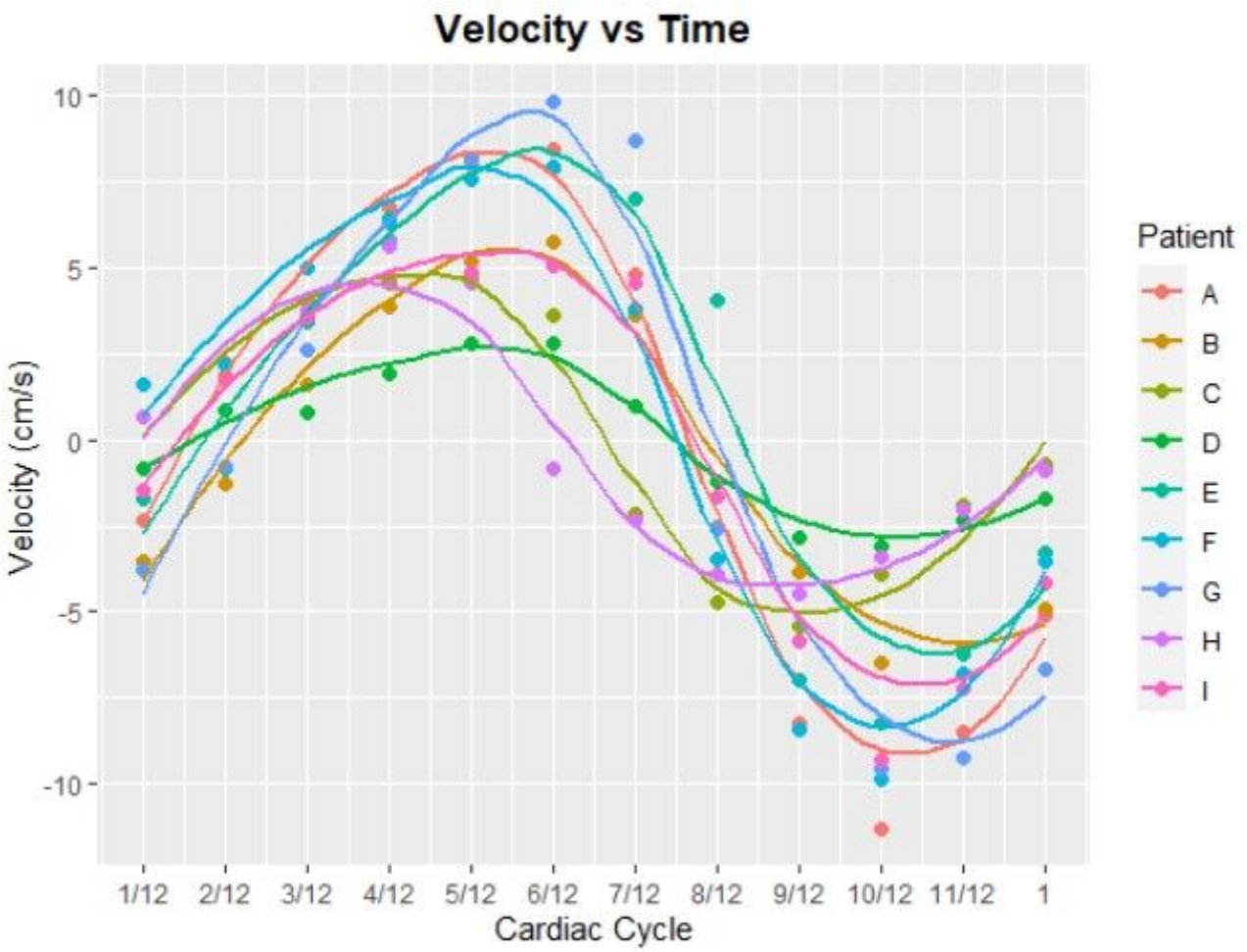

Figure 5

Illustration of the changes in max velocity（cm/s） of the aqueduct throughout the cardiac cycle.

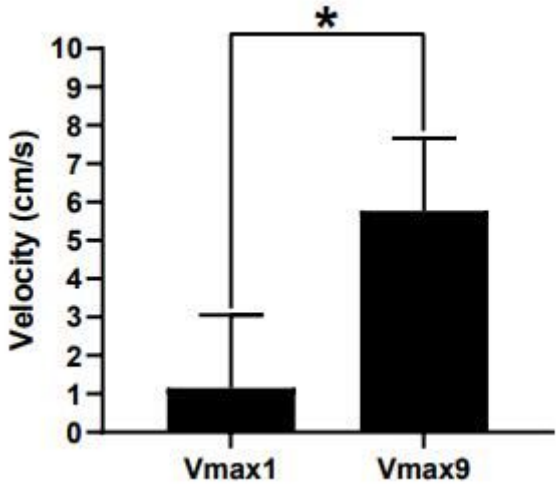

Figure 6

Illustration different results of Vmax1 and Vmax9. Vmax1 was significantly lower than Vmax9. * P < 0.05; ns, not significant.

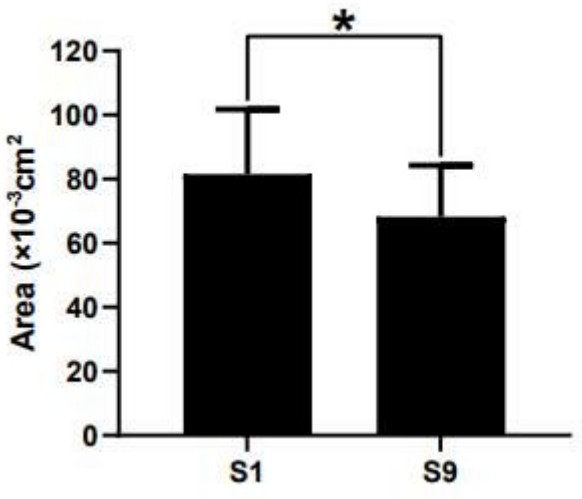

Figure 7

Illustration different results of S1 and S9. Illustration different results of S1 and S9, S1 was significantly higher than S9. * P < 0.05; ns, not significant.

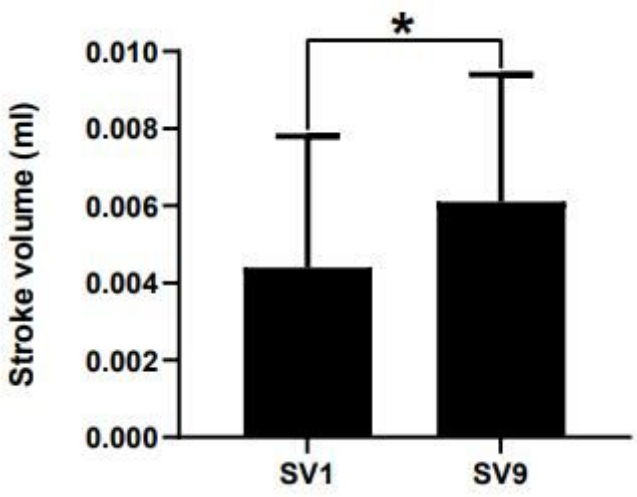

Figure 8

Illustration different results of SV1, and SV9, which uses a unique ROI for each phase of the cardiac cycle. SV1 was significantly lower than SV9. * P < 0.05; ns, not significant.